

Supplemental Information on:

Peyman Falahat, Adrian Goldspink, Lucia Oehler, Jessica Schmitz, Julia Miranda, Islem Gammoudi, Jan Hinrich Bräsen, Niklas Klümper, Olena Babyak, Christian Kurts, Herrmann Haller, Marieta Toma, and Sibylle von Vietinghoff

NaCl and urea modulate CD8⁺ T cell survival, renal accumulation and response to BK virus

Contents:

Supplemental methods

Supplemental Figures 1-16

Supplemental Tables 1-8

Supplemental Methods

Immunostaining and microscopy of kidney tissue

Paraffin sections of murine kidneys was stained with rabbit anti-mouse CD8a (1:1000, Abcam) after heat-pretreatment (pH 9.0, Tris/EDTA buffer), quenching with Peroxidase Suppressor (Thermo Fisher) and blocking with universal blocking buffer (Thermo Fisher) over night at 4 °C followed by HRP-conjugated anti-rabbit IgG (ab6721, Abcam) DAB/Metal staining (Thermo Fisher) using Pierce™ Peroxidase Detection Kit (Thermo Fisher) with hematoxylin counterstain.

Human kidney transplant biopsies were fully re-scored according the Banff 2022 classification by an experienced nephropathologist (JHB)(1). Immunostaining of serial sections with polyclonal rabbit anti-CD3 (Agilent, 1:100), monoclonal rabbit anti-CD4 (SP35, Zytomed Systems, 1:50), monoclonal mouse anti-CD8 (C8/144B, Agilent, 1:50) and monoclonal rat anti-CD209 (h209, LSBio, 1:50) antibodies on heat-pretreated (Zytomed Systems) rehydrated sections (CD3, CD4, CD8: TRIS-EDTA buffer, pH 9; CD209: citrate buffer, pH 6, 98°C, 40 min) using donkey anti-rabbit IgG and donkey anti-mouse IgG (both from Jackson ImmunoResearch) or anti-rat IgG VisUCyte HRP Polymer antibodies (R&D Systems), respectively, after peroxidase blocking (3% H₂O₂) was essentially as described (2). Chromogen detection was performed with 3,3'-diaminobenzidine (Zytomed Systems) and hemalum counterstain. Negative controls omitting primary antibody were included into all staining protocols.

Quantification of renal immune cell infiltrates

Whole slide images were digitized with Aperio CS2 (Leica Biosystems) at 20x magnification for murine and Metafer Scanning Platform (MetaSystems) at 20x magnification for human samples. QuPath (v0.4.4 and 0.5.1) was used for quantitative scan analysis (3, 4). The reviewer of all murine and human histologic stainings was blinded to diuretic therapy and any clinical

data and only given an identification number, scan order was randomized. Human medulla and cortex were identified by the presence and absence of glomeruli, facilitated by frequently visible vasculature between these regions. Identification of murine cortex was similar, inner and outer medulla were distinguished by tubular epithelial structure. Prior to applying a semi-automated positive cell detection approach, each scan was annotated for cortex or medulla using QuPath's wand tool, followed by the “fill-holes” function and a manual artefact check. For positive cell detection, a pixel size of $0.1\mu\text{m}$, a background radius of $6\mu\text{m}$, a sigma of $2\mu\text{m}$, a minimum area of $10\mu\text{m}^2$, and a maximum area of $400\mu\text{m}^2$ were requested. At least 5 positively stained cells were averaged for threshold definition. Scans were analyzed for proportion of stained cells defined by nuclei.

Primary human blood and kidney cell isolation, murine kidney cell isolation, cell culture and hyperosmolar stimulation

Human peripheral blood mononuclear cells from anonymized buffy coats (PBMC) were enriched by density gradient centrifugation with Pancoll 1.077 (PAN-Biotech) as described (5). Normal kidney cortex and medulla tissues were dissected by a certified pathologist (MT) from kidneys of male patients, age 67 (56-73) years, who underwent partial nephrectomy for renal cell cancer at UKB urology department, and cultured immediately after enzymatic digestion as described (6). None of the patients received diuretic therapy at the time of surgery. Non-adherent cells collected after 2h culture in full Roswell Park Memorial Institute (RPMI, 296mOsm/L, 138.4 mM Na^+) 1640 media with GlutaMAX™ (Thermo Fisher Scientific) supplemented with 10%FCS (PAN-Biotech). Outer and inner medulla were dissected and filtered through a $70\mu\text{m}$ cell strainer (Corning). HK2 human tubular epithelial cells (Cell Lines Service) were cultured in full Dulbecco's Modified Eagle Medium: F12 (DMEM, 328mOsm/L, 150.5 mM Na^+ , Lonza) supplemented with 10% FCS and were let to adhere to tissue culture plate for at least 2h prior to addition of PBMC. Co-culture of HK2 cells with blood leukocytes

was in 50% RPMI/50% DMEM (144.4 mM Na⁺). NaCl, urea, Pifithrin (30 μM, Sigma Aldrich, solvent control: DMSO 1:3333) or HgCl₂ (10 μM, Sigma Aldrich, dissolved in PBS), were added in the indicated concentrations. Cells were transferred onto fresh HK2 cells for restimulation. Carboxyfluorescein succinimidyl ester (CFSE, 5 μM, Cayman Chemicals), PepTivator[®] BKV or EBV (10 μl/5+10⁶ cells) and CD8⁺ T Cell Isolation Kit (purity 81±3.7% CD8⁺/CD3⁺ cells in 8 indep. isolations, both: Miltenyi) were employed according to the manufacturers' instructions.

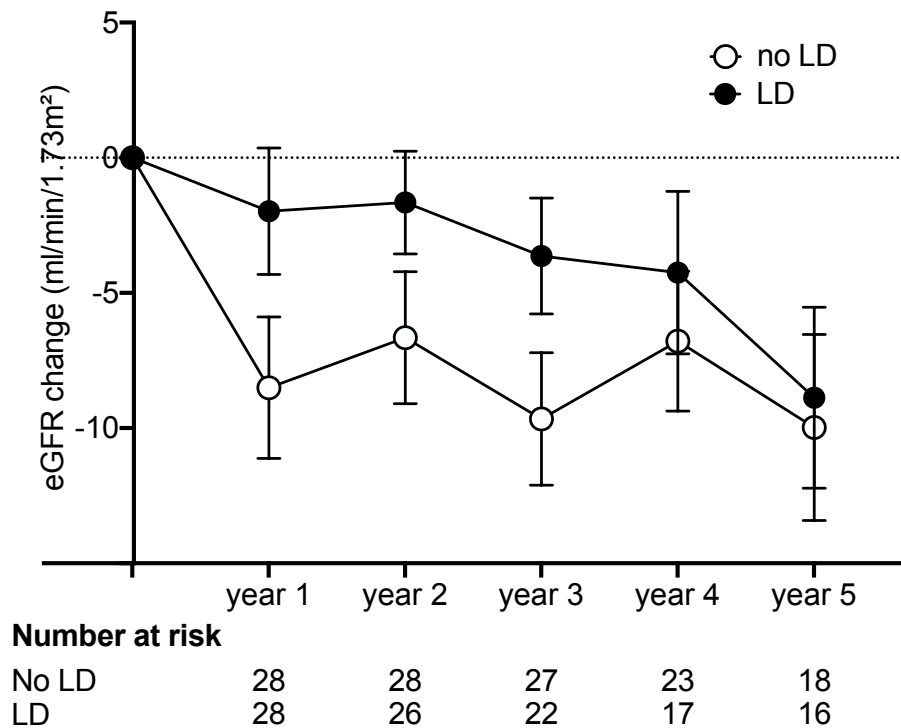
Flow cytometry

The following antibodies were used: anti-mouse: anti-CD3 (17A2), anti-CD4 (GK1.5), anti-CD8 (53-6.7) anti-CD11b (M1/70), anti-CD19 (6D5), anti-CD45 (30-F11) (Biolegend), anti-human: anti-CD3 (HIT3a), anti-CD8 (SK1, HIT8a), anti-CD11b (ICRF44), anti-CD27 (M-T271), anti-CD54 (HA58), anti-CD137 (4B4-1), anti-ITGb7 (FIB504), anti-KLRG1 (SA231A2) (Biolegend). AnnexinV (Biolegend), near-infrared LIVE/DEAD[®] Fixable Dead Cell Stain Kit (both: Invitrogen) and FITC Active Caspase3 Apoptosis Kit (BD Bioscience) were used according to the manufacturers' instructions. Human counts were determined by BD Calibrite[™] APC Beads (BD Bioscience) at a final concentration of 10000 beads/ml, murine kidney cells counts using BD Truecount[™] Tubes (BD Bioscience). Cytokine concentrations were analyzed with LEGENDplex[™] Human inflammation Panel 1 (Biolegend) in supernatants stored at -80°C until analysis. Flow cytometry was performed on a Becton-Dickinson FACSCanto or LSR Fortessa Cell Analyzer (BD Bioscience), cell sorting on a BD FACSAria III Cell Sorter (BD Bioscience) or Sony MA900 Multi-Application Cell Sorter (Sony Biotechnology, San Jose, CA) at 4°C. Data were analyzed using FlowJo software (Tree Star Inc.).

RNA sequencing

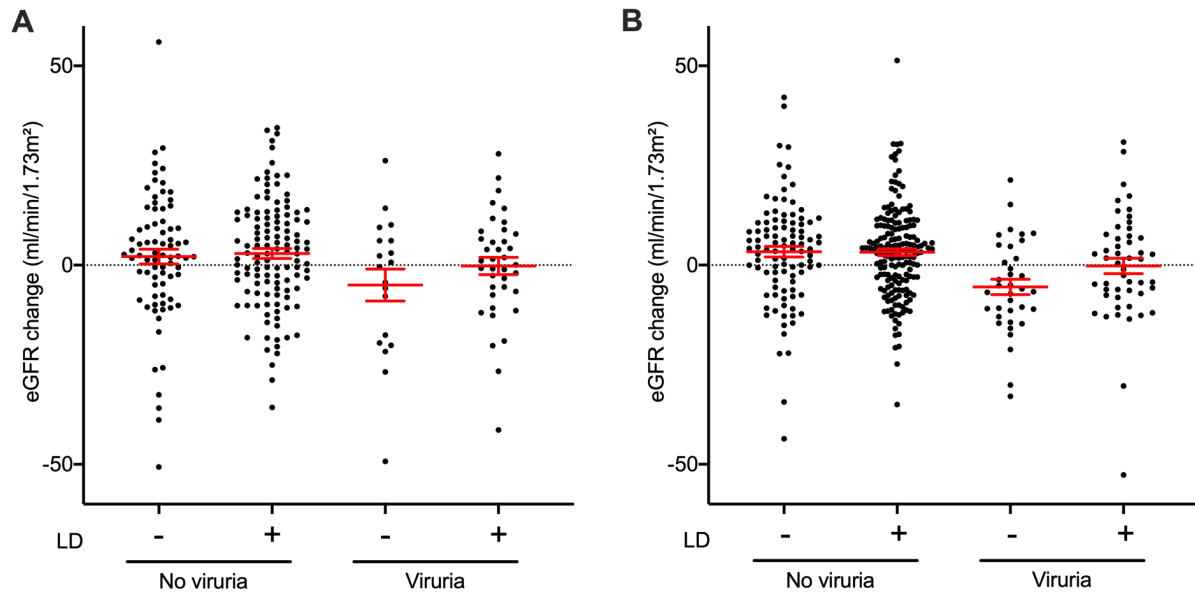
RNA was isolated using NucleoSpin RNA Kit (Macherey-Nagel), yield and purity were determined in a NanoDrop 1000 Spectrophotometer (Thermo Scientific). RNA samples were sequenced at NGS Core Facility Bonn. The 3'mRNA Seq was performed using the Lexogen QuantSeq 3'mRNA FWD Library Prep Kit using 1000ng total RNA as input material. Sequencing was performed on an Illumina NovaSeq 6000 device at 10M reads per sample. Data was processed using nf-core/rnaseq v3.14.0 (doi: <https://doi.org/10.5281/zenodo.1400710>) of the nf-core collection of workflows (7), utilising reproducible software environments from the Bioconda (8) (and Biocontainers (9) projects. The pipeline was executed with Nextflow v24.04.2(10) with the following command: `nextflow run nf-core/rnaseq -profile docker -params-file params_human.yaml`.

Supplemental Figures:



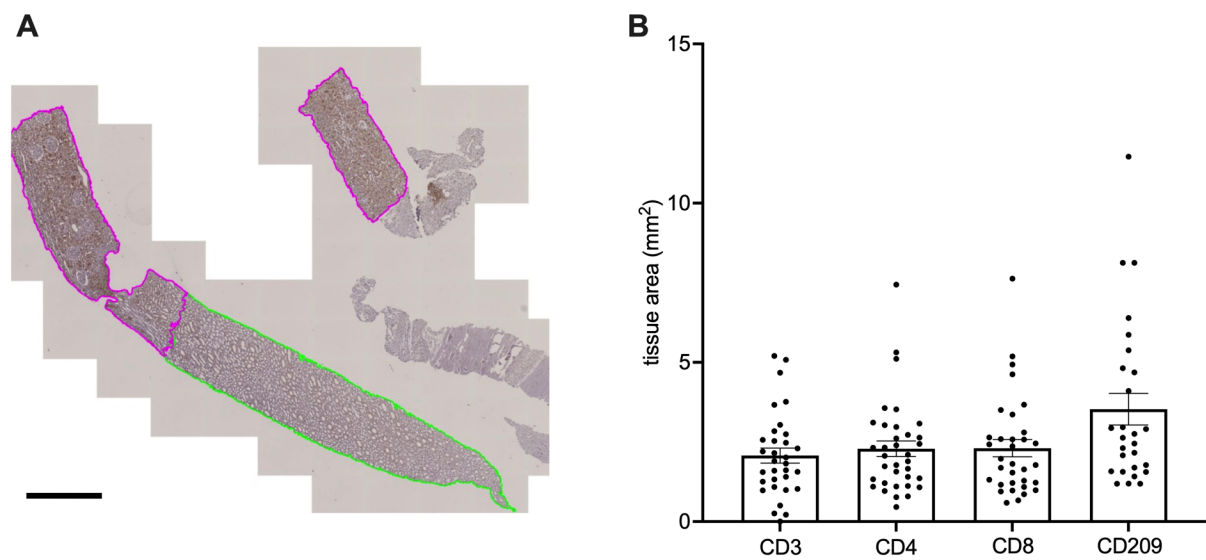
Supplemental Figure 1: eGFR development after diagnosis of BK viremia

The change in eGFR calculated by the creatinine-based CKD-EPI formula in patients clinically diagnosed as BKV (i.e. viremia) during the first twelve month over five years after kidney transplantation according to loop diuretic (LD) use (indicated with black versus white circles, stacked mixed-effects ANOVA: significant for time ($p < 0.0001$), non-significant for LD use ($p = 0.154$)). Number of patients at risk is indicated at the bottom of the figure, whiskers indicate SEM.



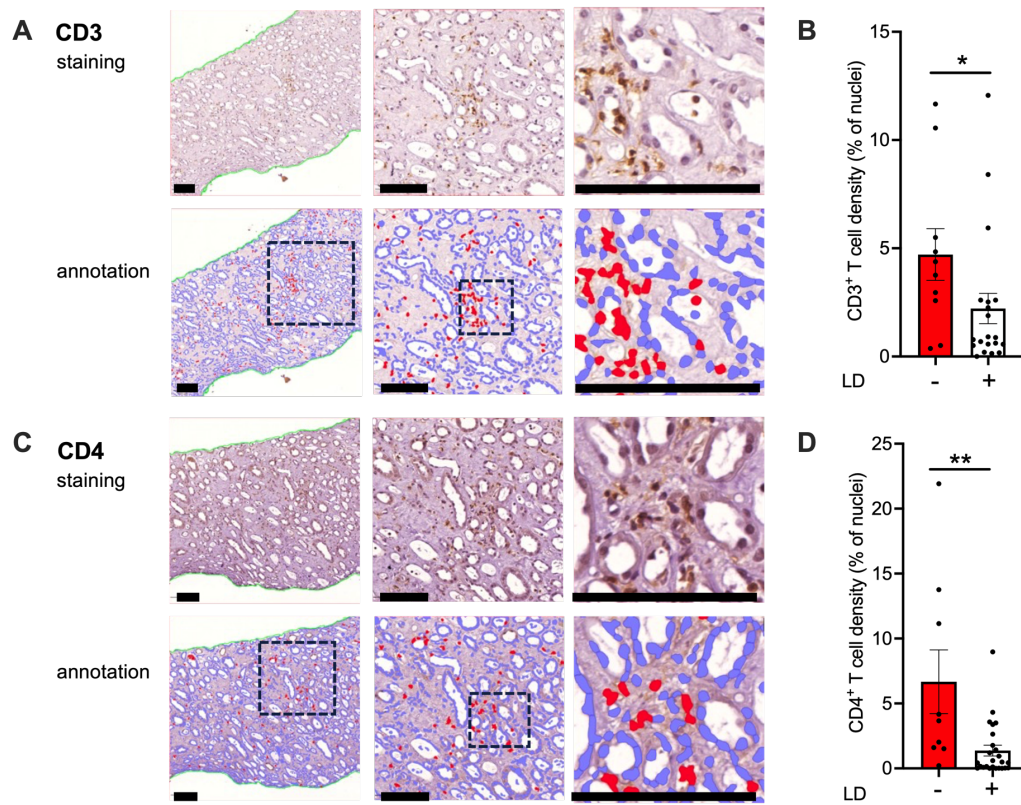
Supplemental Figure 2: eGFR development with and without viruria and loop diuretic therapy in females and males

(A,B) eGFR development during the first year after kidney transplantation in the subgroups of female (A) and male (B) patients with and without BK viruria and loop diuretic (LD) therapy.



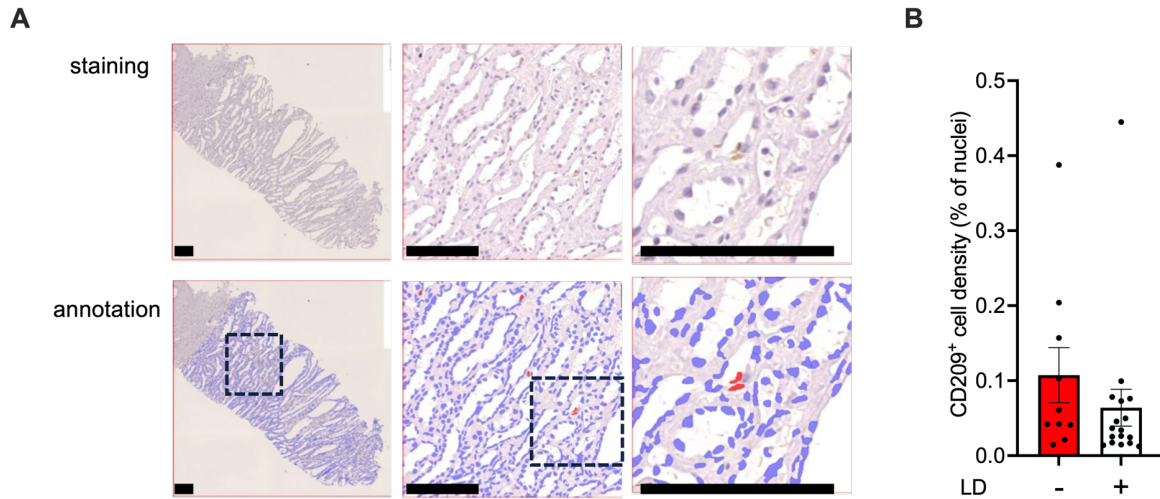
Supplemental Figure 3: Quantification of medullary areas in whole slide scans of kidney biopsies

(A-C) Renal cortex (pink) and medulla (green) were annotated on whole-slide scans of the kidney-biopsy specimen (A, size bar indicates 1mm). (B) Size of medullary tissue areas that were evaluated for each patient and staining (Dunn's).



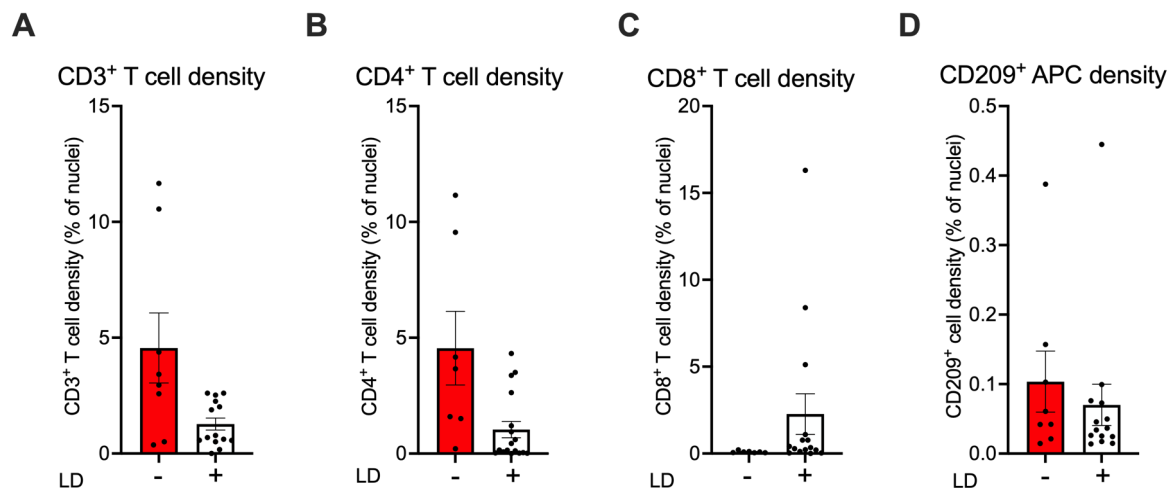
Supplemental Figure 4: Loop diuretic therapy association with T cell densities in the renal allograft

(A-D) Total CD3⁺ (A,B) and CD4⁺ helper (C,D) densities in three-month post-implantation biopsies of kidney allografts according to loop diuretic (LD) use (A,C examples of stainings and annotations of typical sections, bars indicate 100µm, B,D statistical analysis by Mann-Whitney tests).



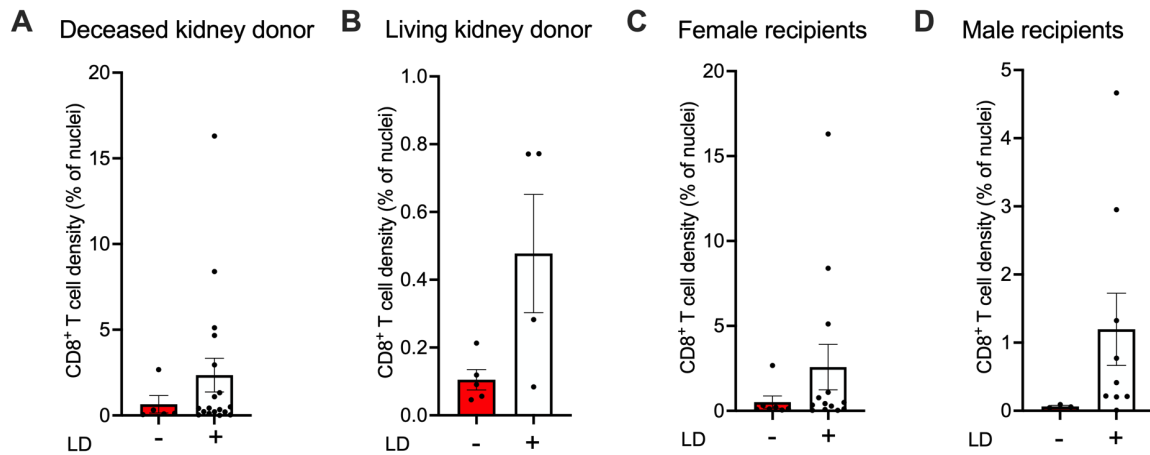
Supplemental Figure 5: Role of loop diuretic therapy for CD209⁺ antigen presenting cell densities in the renal allograft

(A,B) DC-SIGN (CD209)⁺ antigen presenting cell densities in three-month post-implantation biopsies of kidney allografts according to loop diuretic (LD) use (A, examples of stainings and annotations of typical sections, bars indicate 100μm, and B, statistical analysis by Mann-Whitney test).



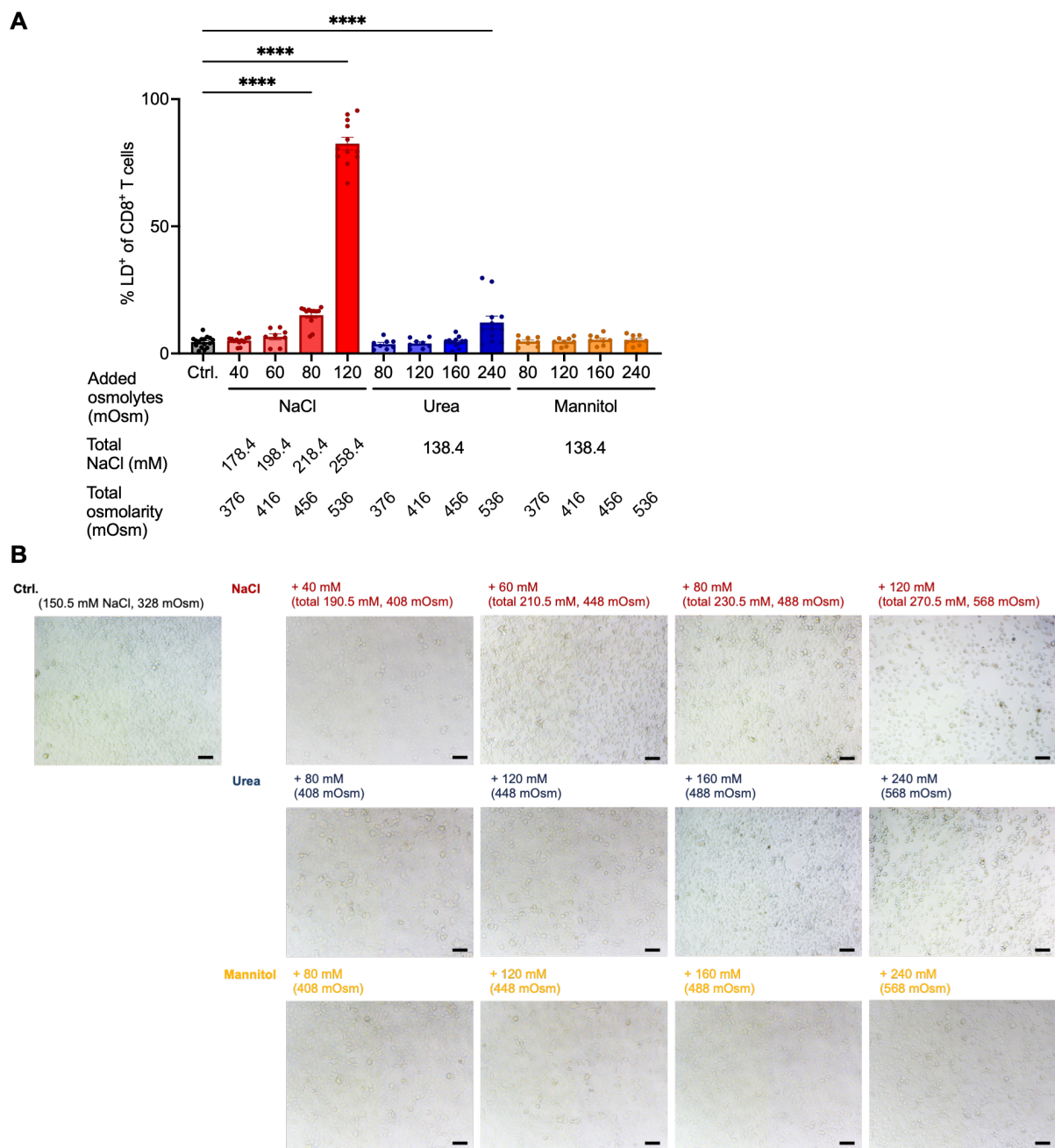
Supplemental Figure 6: Renal medullary leukocyte densities in the absence of rejection

(A-D) Densities of total CD3⁺ (A) and CD4⁺ helper (B), CD8⁺ cytotoxic T cells (C) and CD209⁺ antigen presenting cells (D) in biopsies without rejection or borderline rejection diagnosis according to loop diuretic (LD) use.



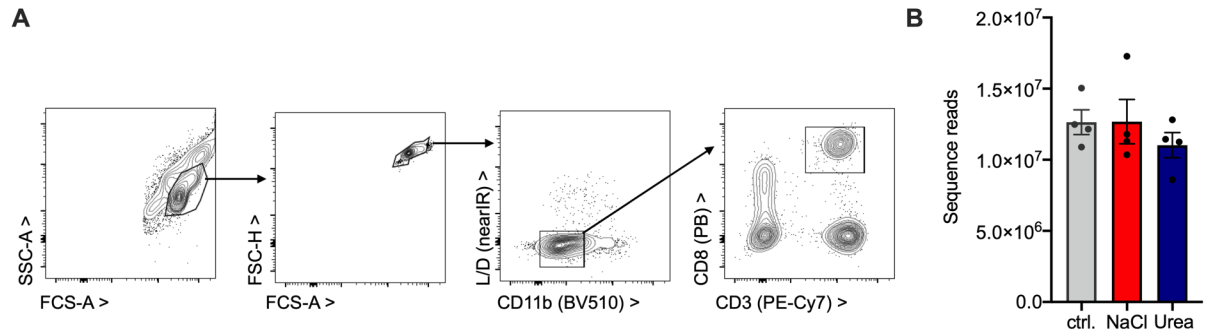
Supplemental Figure 7: Renal medullary CD8⁺ T cell densities depending on graft provenience and recipient gender

(A,B) Densities of CD8⁺ cytotoxic T cells in biopsies from deceased (A) and living donor (B) kidneys and (C,D) Densities of CD8⁺ cytotoxic T cells in biopsies from grafts transplanted into female (A) and male (B) recipients according to loop diuretic (LD) use separately.



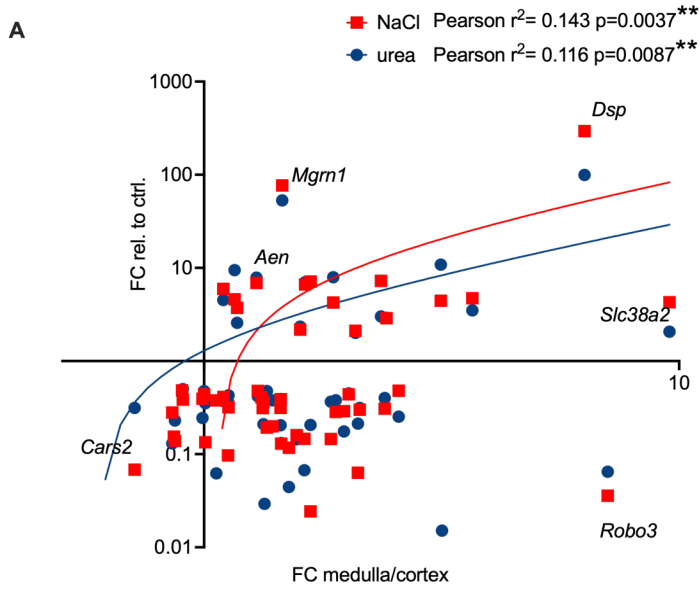
Supplemental Figure 8: T cell and tubular epithelial cell survival in elevated NaCl and urea

(A) Human adhesion depleted PBMC were cultured with allogenic stimulation by HK2 human tubular epithelial cells with and without addition of NaCl and urea or mannitol tonicity control in full RPMI media in the indicated concentrations resulting in the indicated total osmolarities. The proportion of dead (LD⁺) CD8⁺ T cells was enumerated by flow cytometry on day three (n=12 from 6 donors in 5 indep. experiments, Dunnett's after ANOVA). (B) HK2 cells were cultured for 20h with or without additional NaCl and urea or mannitol tonicity control in full DMEM media resulting in the indicated total osmolarities. Representative images of one of four experiments (bars indicate 100μm).



Supplemental Figure 9: Sorting for and read counts of CD8⁺ T cell RNA sequencing

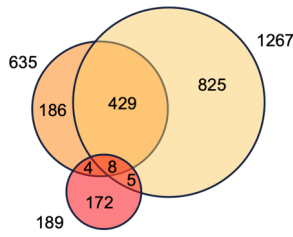
(A) Gating strategy of flow cytometric live CD8⁺ T cell sorting. CD8⁺CD3⁺CD11b⁻LD⁻ cells were selected for RNA isolation. **(B)** Sequence read counts did not differ between the three experimental groups (ANOVA).



Supplemental Figure 10: Gene regulation correlation with the renal cortico-medullary gradient

Correlation of fold-change (FC) expression change of genes commonly regulated by NaCl and urea (n=72, defined in Figure 4F) with relative expression in healthy murine medulla versus cortex (n=3, GSE8174136, (11)).

A Upregulated genes



Naive CD8⁺ T cells on α CD3/ α CD28, d5

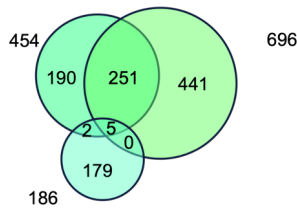
Scirgolea et al., NI 2024

Soll et al., NI 2024

Total CD8⁺ T cells on allogenic TEC, 72+6h

Present dataset

B Downregulated genes



Naive CD8⁺ T cells on α CD3/ α CD28, d5

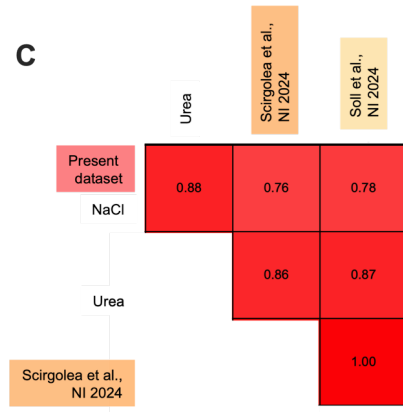
Scirgolea et al., NI 2024

Soll et al., NI 2024

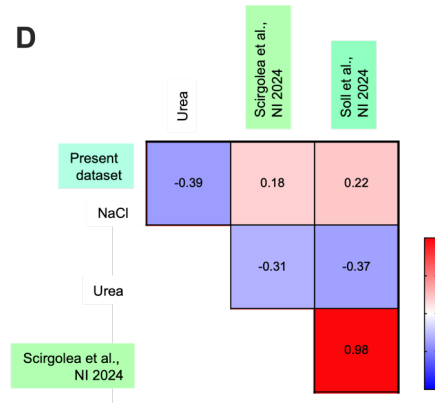
Total CD8⁺ T cells on allogenic TEC, 72+6h

Present dataset

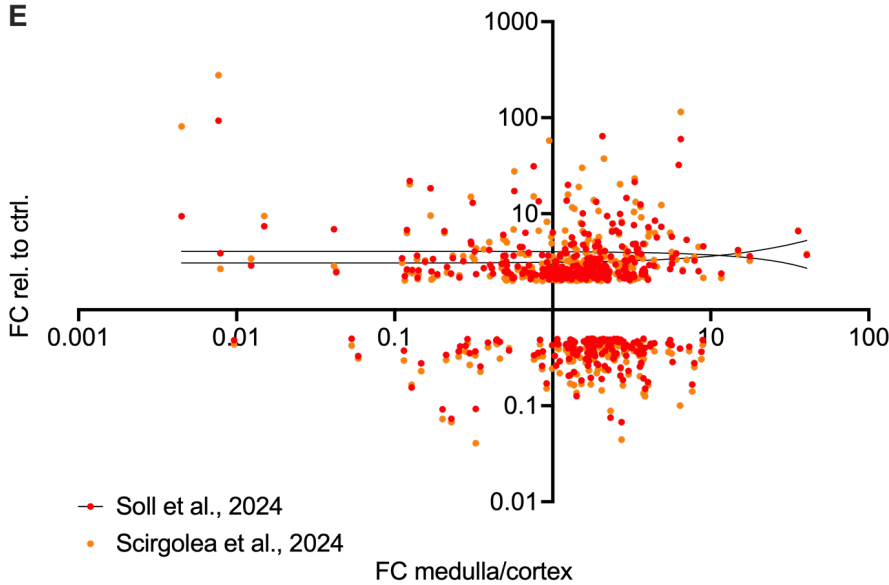
C



D

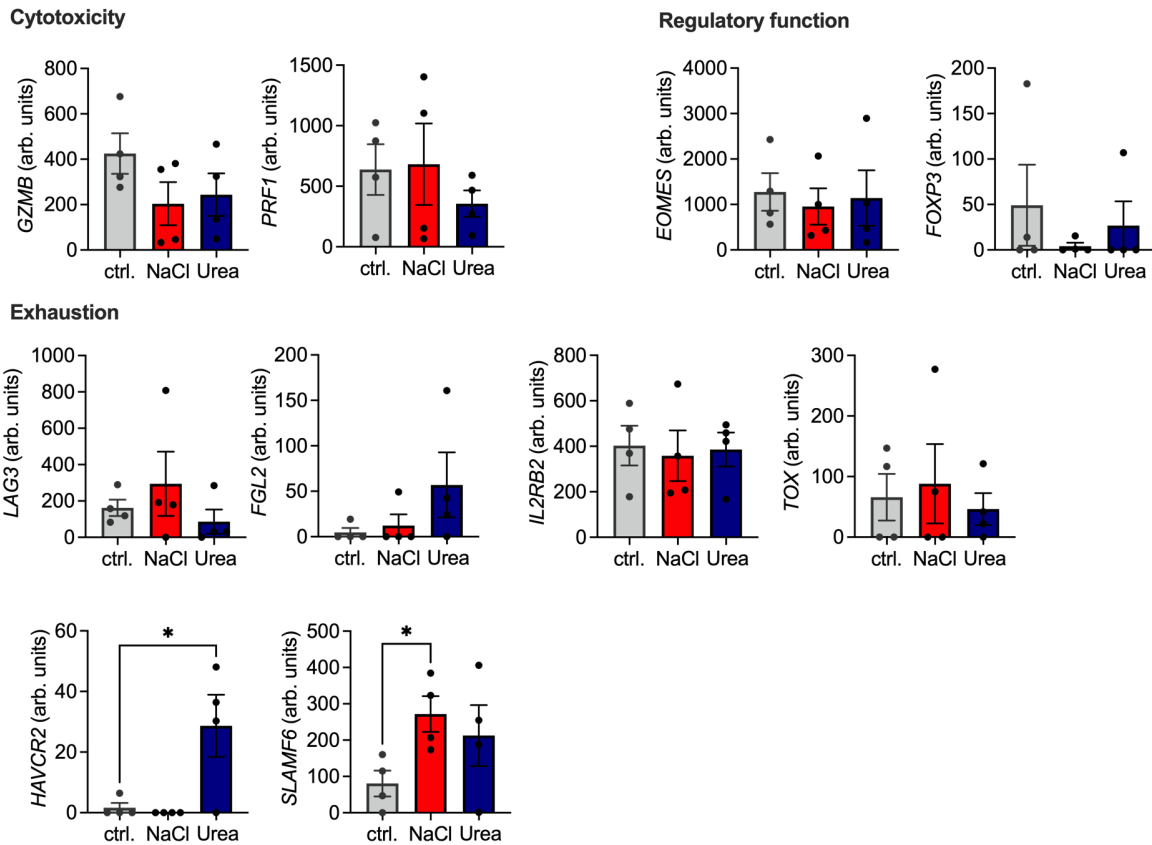


E



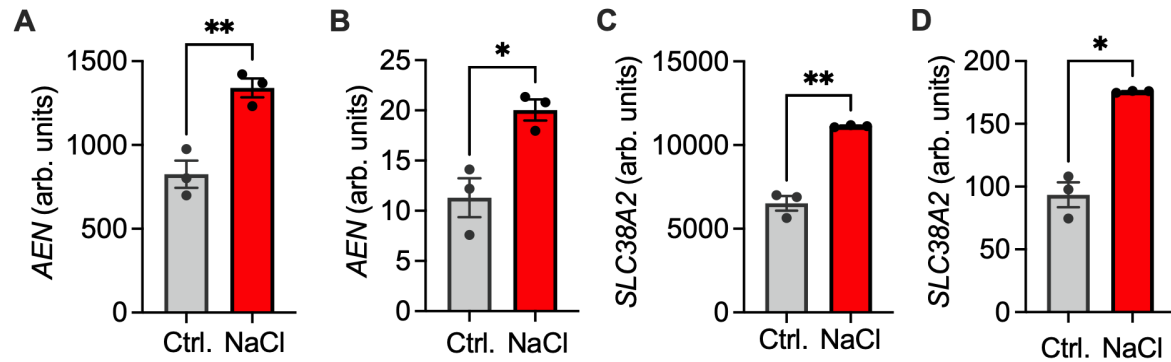
Supplemental Figure 11: CD8⁺ T cell gene regulation in comparison to the kidney cortico-medullary gene expression profile

(A-E) Gene expression profiles of published human naïve CD8⁺ T cells stimulated with anti-CD3 and anti-CD28 with (12) or without (13) exogenous IL-2 in the absence and presence of additional 80 mmol (12) or 67 mmol (13) NaCl were compared with each other, our results in allogenic-restimulated total CD8⁺ T cells and renal gene expression gradients. (A,B) Overlapping gene regulation among up- (A) and downregulated genes is visualized using Venn's diagram including genes with an at least twofold change. (C,D) Extent of up- (C) and downregulation (were) compared (Pearson's r , significance level obtained in all tests in C, and the downmost in D). (E) Correlation of gene regulation magnitude with the renal cortico-medullary gene expression gradient (11) for all commonly regulated genes in (12) and (13). No significant correlation was found (Pearson's test).



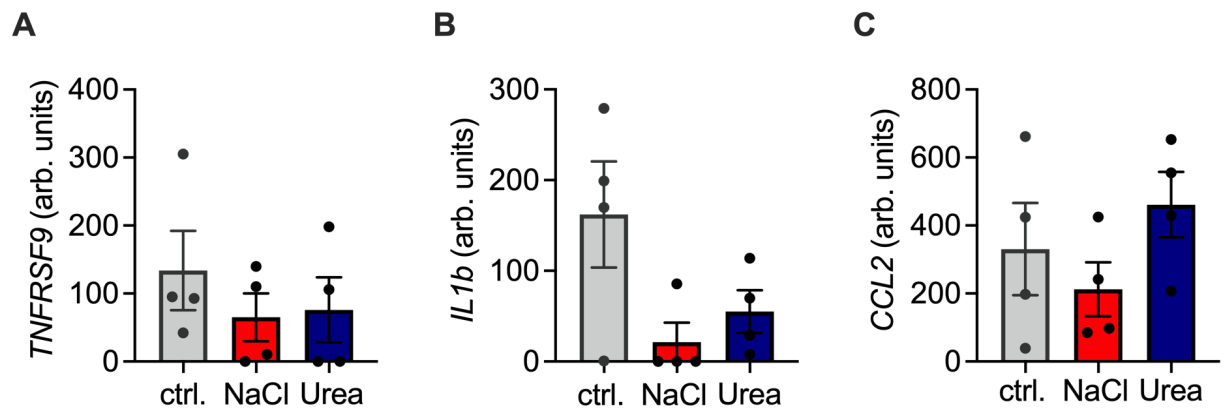
Supplemental Figure 12: Regulation of renal T cell activation marker expression by NaCl and urea

Markers used characterize T cell cytotoxicity, exhaustion and regulatory function in a recent study on chronic alloimmune response in the kidney,(14) and exhaustion markers *HAVCR2* (protein: Tim3) and *SLAMF6* were assessed in CD8⁺ T cells isolated by flow cytometry by RNA sequencing as described in Figure 9 (n=4 donors, t-tests).



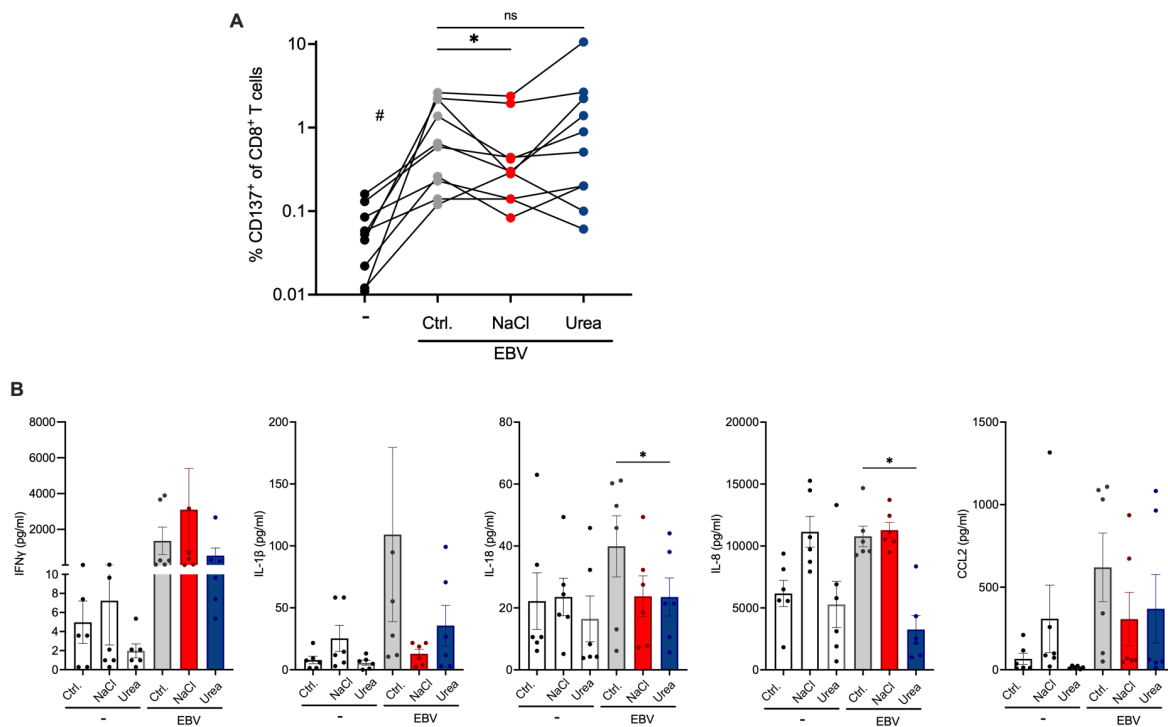
Supplemental Figure 13: AEN and SLC38A2 regulation in naive CD8⁺ T cells

(A-D) AEN (A,B) and SLC38A2 (C,D) gene expression profiles in human naive CD8⁺ T cells stimulated with anti-CD3 and anti-CD28 with(12) (A,C) or without(13) (B,D) exogenous IL-2 in the absence and presence of additional 80 mmol(12) or 67 mmol(13) NaCl (t-tests with Welch's correction).



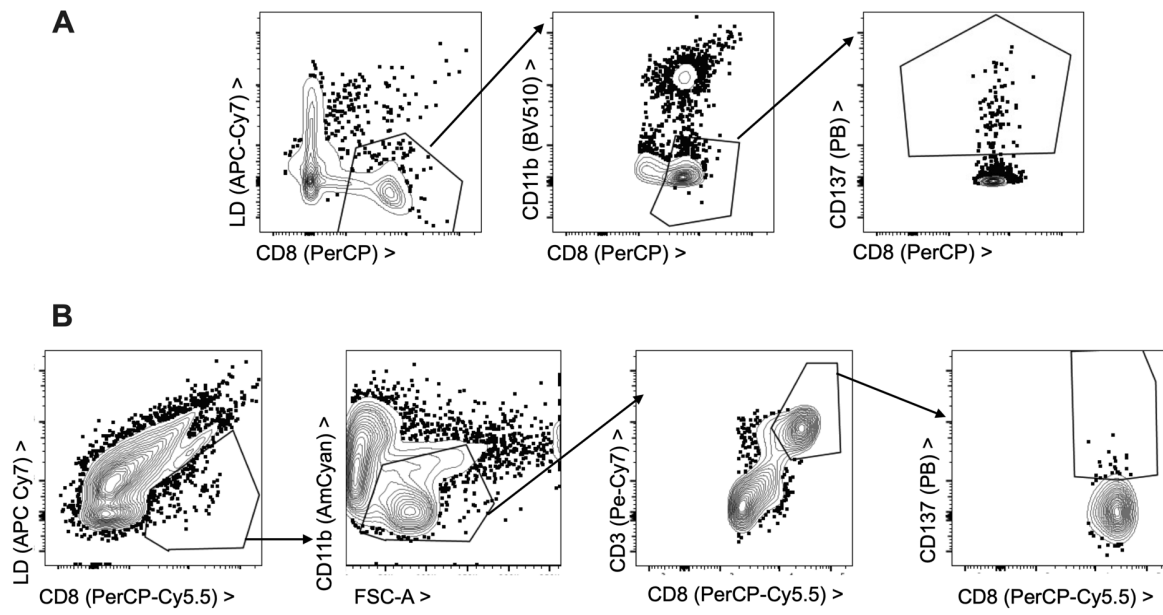
Supplemental Figure 14: Markers of T cell activation in CD8⁺ T cell RNA sequencing

(A-C) The CD137- coding gene *TNFRSF9* (A), *IL1B* (B) and *CCL2* (C) gene expression in isolated live CD8⁺ T cells subjected to RNA sequencing (n=4 donors) as described in Figure 4. *IFNG*, *TNFA*, *IL8*, *IL10* and *IL18* were below detection limit.



Supplemental Figure 15: Response to EBV-peptide is dampened by environmental NaCl

(A,B) PBMC were cultured with and without stimulation with EBV peptide in the absence or presence of additional 80 mM NaCl, equimolar 160 mM urea, or control for three days (A) The proportion of responsive CD137^{HIGH}CD8⁺ T cells was quantified by flow cytometry (gating in Supplemental Figure 9A, statistical analysis of n=10 from 5 donors in 3 indep. experiments, #paired t-test of stimulation, *Dunn's after ANOVA of peptide conditions). (B) Supernatant IFN γ , IL-1 β , IL-18, IL-8, and CCL2 was assessed by cytometric bead assay (n=5 T cell donors in independent experiments, Dunn's of peptide conditions).



Supplemental Figure 16: Human CD8⁺ T cell gating strategies

(A,B) Live CD8⁺CD11b⁻ cells were gated from human PBMC (A) and live CD8⁺CD3⁺CD11b⁻ healthy human kidney tissues (B) to assess activation marker CD137 expression.

Supplemental Tables:

Supplemental Table 1: Therapy and outcome of BK viremic patients according to loop diuretic use

| | No loop diuretic (n=35) | Loop diuretic (n=31) | p-value |
|---|------------------------------------|---------------------------------|----------------|
| BKV | | | |
| Maximal viral load (urine, IU/ml) | 2.2±4.2*10 ⁷ | 8.3±17*10 ⁷ | 0.45 |
| Maximal viral load (plasma, IU/ml) | 3.9±8.1*10 ⁵ | 4.2±8.4*10 ⁵ | 0.96 |
| Kidney biopsy with BKVn if performed | 17% (2/12) | 24% (6/25) | 0.70 |
| Therapeutic measures | | | |
| Mycophenolate dose reduction | 97% (30/31) | 86% (25/29) | 0.19 |
| Switch from mycophenolate to mTOR inhibitor | 39% (12/31) | 65% (17/26) | 0.06 |
| Calcineurin inhibitor cessation | 30% (9/30) | 40% (10/25) | 0.57 |
| High dose intravenous immunoglobulin | 13% (4/31) | 17% (5/29) | 0.73 |
| Renal function | | | |
| eGFR (ml/min/1.73m ²) at first outpatient visit | 51.1±15 | 38.5±14 | 0.0029* |

Therapeutic measures within two years after diagnosis are included.

Means±SD, Mann-Whitney tests for exploratory p-values.

Supplemental Table 2: eGFR development according to loop diuretic therapy, rejection status and BKV reactivation

| eGFR change | No LD | | LD | | p-value |
|----------------------|---------------------------|-----|---------------------------|-----|---------|
| | ml/min/1.73m ² | n | ml/min/1.73m ² | n | |
| All | | | | | |
| All | 0.88±15 | 231 | 2.3±13 | 386 | 0.33 |
| No BKV | 2.8±15 | 176 | 3.1±12 | 198 | 0.87 |
| Viruria | -5.3±14 | 55 | -0.2±13 | 88 | 0.02* |
| Viruria and viremia | -6.3±11 | 29 | -3.2±15 | 30 | 0.17 |
| No rejection | | | | | |
| All | 1.1±15 | 163 | 2.7±13 | 276 | 0.29 |
| No BKV | 3.2±15 | 127 | 3.2±12 | 221 | 0.78 |
| Viruria | -8.0±16 | 13 | 1.7±14 | 38 | 0.086 |
| Viruria and viremia | -6.6±10 | 23 | -1.7±17 | 17 | 0.15 |
| Any rejection | | | | | |
| All | 0.4±14 | 68 | 1.4±12 | 110 | 0.84 |
| No BKV | 1.8±13 | 49 | 2.8±12 | 77 | 0.85 |
| Viruria | -0.3±16 | 13 | 0.6±8.5 | 10 | 0.96 |
| Viruria and viremia | -9.2±14 | 6 | -5.2±12 | 13 | 0.32 |

LD indicates loop diuretic therapy. Mean±SD, Mann-Whitney tests for exploratory p-values.

Supplemental Table 3: Characterization of the kidney graft recipients of the biopsy cohort

| | No loop diuretic (n=21) | Loop diuretic (n=44) | p-value |
|--|---------------------------------|--------------------------------|-----------|
| Basic characteristics | | | |
| Age (years) | 46±17 | 54±13 | 0.042* |
| Gender | 57% (12) male | 49% (22) male | 0.6 |
| Graft characteristics | | | |
| Cold ischemia time (min) | 453±362 | 751±420 | 0.0078** |
| Delayed graft function | 0% (0) | 20% (9) | 0.0475* |
| Living donor | 52% (11) | 9% (4) | 0.0003*** |
| HLA mismatch (A, B, DR) | 3.1±2.3 | 2.6±1.6 | 0.28 |
| ABOi graft | 19% (4) | 2% (1) | 0.036* |
| Immunosuppression at first outpatient visit | | | |
| CNI | 100% (21) | 99% (42) | 0.52 |
| Cyclosporine A | 19% (4) | 33% (15) | 0.26 |
| Tacrolimus | 81% (17) | 67% (30) | 0.26 |
| mTOR inhibitor | 0% (0) | 0% (0) | 1 |
| Loop diuretic dose (mg) | 0 | 69±46 | <0.001*** |
| Graft function at first outpatient visit | | | |
| eGFR CKD-EPI (creatinine) | 55±18 ml/min/1.73m ² | 35±15ml/min/1.73m ² | <0.001*** |
| Proteinuria (g/day) | 0.1±0.11 | 0.1±0.08 | 0.87 |
| Biopsy characteristics | | | |
| Time after Ktx (days) | 92.1±27.1 | 93.2±18.4 | 0.87 |

Values are expressed as % (n) or mean±SD. Student's t-test or Mann-Whitney test non-normally distributed variables was employed to obtain exploratory p-values. >90% of patients in both groups received basiliximab for induction, low dose steroids and mycophenolate. Loop diuretic dose is given as mg furosemide or equivalent.

Supplemental Table 4: Histologic characterization of allograft biopsies with and without loop diuretic exposure

| | No loop diuretic (n=21) | Loop diuretic (n=44) | p-value |
|--|-------------------------|----------------------|---------|
| Banff classification | | | |
| Any rejection | 24% (5) | 25% (11) | 1 |
| Normal (Banff cat. 1) | 0% (0) | 0% (0) | 1 |
| Antibody mediated rej. (Banff cat. 2) | 0% (0) | 2% (1) | 1 |
| Cellular borderline rej. (Banff cat. 3) | 14% (3) | 14% (6) | 1 |
| T cell mediated rej. (Banff cat. 4) | 9.5% (2) | 8% (4) | 1 |
| BKV nephropathy | 4.7% (1) | 0% (0) | 1 |
| i (interstitial infiltrate in non-fibrotic cortex) | 0.4±0.8 | 0.3±0.7 | 1 |
| t (tubulitis) | 0.4±0.8 | 0.5±0.9 | 0.46 |
| v (arterial endotheliatis) | 0±0 | 0.05±0.3 | 1 |
| g (glomerulitis) | 0±0 | 0.02±0.17 | 1 |
| ptc (peritubular capillaritis) | 0±0 | 0.05±0.32 | 1 |
| C4d | 0.5±1.1 | 0.02±0.16 | 0.028* |
| ci (cortical fibrosis) | 0.6±0.6 | 0.8±0.7 | 0.4 |
| ct (atrophic cortical tubuli) | 1±0.3 | 1.1±0.4 | 0.26 |
| cv (arterial stenosis) | 0.05±0.2 | 0.2±1.4 | 1 |
| cg (transplant glomerulopathy) | 0±0 | 0±0 | 1 |
| ti (interstitial infiltrate total cortex) | 0.5±0.8 | 0.7±0.8 | 0.32 |
| i-IFTA (interstitial fibrosis and tubular atrophy) | 1.4±1.3 | 1.7±1.1 | 0.20 |
| t-IFTA (interstitial fibrosis and tubular atrophy) | 0.6±0.7 | 0.8±0.7 | 0.20 |
| pvl (polyoma virus lesions) | 0±0 | 0±0 | 1 |
| ah (arterial hyalinosis) | 0.6±0.7 | 0.8±0.7 | 0.19 |
| mm (mesangial matrix expansion) | 0.05±0.2 | 0.2±0.5 | 0.37 |
| Banff cat. 6 type damage | 71% (15) | 68% (30) | 1 |
| Tubular damage | 71% (15) | 68% (30) | 1 |
| CNI toxicity | 4.7% (1) | 16% (7) | 0.27 |

Values are expressed as % (n) or mean±SD. Mann-Whitney test was employed for exploratory p-values.

Supplemental Table 5: Compartmental CD8⁺ T cell densities and assessed areas in patients with and without histologic rejection

| CD8 | No LD | | LD | | p-value | |
|-----------------------------|-------------------------|-----------------|-------------------------|-----------------|---------|-----------------|
| | Area (mm ²) | Nuclear density | Area (mm ²) | Nuclear density | area | Nuclear density |
| All samples (n=65) | | | | | | |
| Cortex | 0.34±0.2 | 0.84±2.5 | 0.35±0.2 | 2.8±4 | 0.563 | 0.0001*** |
| Medulla | 0.29±0.15 | 0.38±0.8 | 0.21±0.15 | 2.0±3.8 | 0.084 | 0.043* |
| No rejection (n=49) | | | | | | |
| Cortex | 0.27±0.17 | 0.87±2.8 | 0.11±0.44 | 2.9±4.7 | 0.14 | 0.0007*** |
| Medulla | 0.32±0.17 | 0.09±0.06 | 0.21±0.17 | 2.27±4.5 | 0.09 | 0.046* |
| Any rejection (n=16) | | | | | | |
| Cortex | 0.54±0.16 | 0.75±0.91 | 0.45±0.23 | 2.2±1.3 | 0.32 | 0.05 |
| Medulla | 0.22±0.11 | 1.0±1.4 | 0.19±0.09 | 1.4±1.7 | 0.66 | 0.66 |

“LD” indicates loop diuretic therapy. Mean±SD, Mann-Whitney tests for exploratory p-values.

Supplemental Table 6: Commonly up-regulated genes in NaCl and urea stimulated CD8⁺ T cells

| gene_id | gene_name | average ctrl | average NaCl | average urea | FC NaCl | p NaCl | FC urea | p urea |
|-----------------|-----------|--------------|--------------|--------------|------------|------------|------------|------------|
| ENSG00000116731 | PRDM2 | 228,770958 | 483,6162 | 458,856675 | 2,11397549 | 0,01304221 | 2,00574705 | 0,01026412 |
| ENSG00000106443 | PHF14 | 180,032286 | 391,93092 | 421,494984 | 2,17700352 | 0,0412999 | 2,34121887 | 0,00751299 |
| ENSG00000061938 | TNK2 | 78,0528125 | 225,192826 | 227,657847 | 2,88513403 | 0,00602622 | 2,91671549 | 0,00768127 |
| ENSG00000129084 | PSMA1 | 95,8126871 | 356,058121 | 246,821015 | 3,7161897 | 0,02859725 | 2,57607863 | 0,0240331 |
| ENSG00000167325 | RRM1 | 48,5490597 | 205,744164 | 385,759525 | 4,23786095 | 0,0429676 | 7,94576717 | 0,0072082 |
| ENSG00000134294 | SLC38A2 | 224,74655 | 961,319049 | 463,440062 | 4,2773473 | 0,02482109 | 2,0620564 | 0,03956366 |
| ENSG00000148841 | ITPRIP | 14,1744585 | 62,9812456 | 153,819811 | 4,44329113 | 0,02022478 | 10,8519004 | 0,01621033 |
| ENSG00000115317 | HTRA2 | 9,89774558 | 45,5403828 | 93,7941392 | 4,60108642 | 0,02431749 | 9,47631342 | 0,00919743 |
| ENSG00000069849 | ATP1B3 | 107,445526 | 507,460952 | 375,586467 | 4,72296029 | 0,01708371 | 3,49559895 | 0,02055776 |
| ENSG00000213983 | AP1G2 | 16,9822021 | 100,804889 | 76,610747 | 5,93591386 | 0,01382321 | 4,5112375 | 0,02317554 |
| ENSG00000247400 | DNAJC3-DT | 19,001528 | 114,995528 | 94,1907534 | 6,05190952 | 0,04343344 | 4,95700944 | 0,04172474 |
| ENSG00000151466 | SCLT1 | 20,3557237 | 135,033028 | 142,937159 | 6,63366383 | 0,00091895 | 7,02196402 | 0,03238349 |
| ENSG00000181026 | AEN | 25,9968553 | 178,607969 | 204,202657 | 6,87036824 | 0,00545698 | 7,8548984 | 0,02614151 |
| ENSG00000170234 | PWWP2A | 37,3358825 | 266,528926 | 262,096615 | 7,13868022 | 0,00237442 | 7,01996571 | 0,02449837 |
| ENSG00000181555 | SETD2 | 63,422181 | 459,43558 | 190,551041 | 7,24408358 | 0,0057221 | 3,00448578 | 0,03412054 |
| ENSG00000253276 | CCDC71L | 5,278252 | 63,8089114 | 82,3160414 | 12,0890233 | 0,01530359 | 15,5953223 | 0,00086818 |
| ENSG00000174839 | DENND6A | 1,00139731 | 53,0944698 | 84,1847993 | 53,0203839 | 0,04644623 | 84,0673312 | 0,01223202 |
| ENSG00000102858 | MGRN1 | 0,99761537 | 76,6551312 | 52,9162736 | 76,8383625 | 0,01258284 | 53,0427612 | 0,00386955 |
| ENSG00000196754 | S100A2 | 0,20027946 | 38,8095398 | 53,6032701 | 193,776933 | 0,04431073 | 267,642371 | 0,01532454 |
| ENSG00000096696 | DSP | 0,20564093 | 60,5445654 | 20,4370401 | 294,418849 | 0,04587016 | 99,3821625 | 0,03048677 |

Supplemental Table 7: Commonly down-regulated genes in NaCl and urea stimulated CD8⁺

T cells

| gene_id | gene_name | ave ctrl | ave nacl | ave urea | FC nacl | p nacl | fc urea | p urea |
|-----------------|-----------|------------|------------|------------|------------|------------|------------|------------|
| ENSG00000154134 | ROBO3 | 121,435517 | 4,3411053 | 7,85582158 | 0,03574823 | 8,5529E-05 | 0,0646913 | 0,0001995 |
| ENSG00000155660 | PDIA4 | 228,028619 | 22,121732 | 83,0033583 | 0,09701296 | 0,00027173 | 0,36400413 | 0,01790465 |
| ENSG00000182154 | MRPL41 | 371,977874 | 143,06812 | 185,605199 | 0,3846146 | 0,00065378 | 0,49896839 | 0,02794397 |
| ENSG00000140694 | PARN | 579,143053 | 181,25057 | 266,427379 | 0,31296338 | 0,00067836 | 0,46003725 | 0,02640504 |
| ENSG00000100258 | LMF2 | 149,300584 | 0 | 4,36434532 | 0 | 0,00093258 | 0,02923194 | 0,00117988 |
| ENSG00000141506 | PIK3R5 | 260,792936 | 50,2358228 | 124,294367 | 0,19262724 | 0,00147839 | 0,47660174 | 0,02152584 |
| ENSG00000088766 | CRLS1 | 87,7897428 | 12,7866117 | 32,0705095 | 0,14565041 | 0,0018092 | 0,36531044 | 0,04590753 |
| ENSG00000118972 | FGF23 | 52,329315 | 22,9794267 | 24,8597745 | 0,43913104 | 0,00190411 | 0,47506402 | 0,00506719 |
| ENSG00000165591 | FAAH2 | 107,529385 | 13,0233159 | 0 | 0,12111402 | 0,00200936 | 0 | 0,0001459 |
| ENSG00000139193 | CD27 | 416,252457 | 169,066021 | 174,65056 | 0,40616222 | 0,00328885 | 0,41957845 | 0,03326989 |
| ENSG00000132478 | UNK | 129,227576 | 8,15067323 | 27,5342502 | 0,06307224 | 0,00344941 | 0,21306792 | 0,03515166 |
| ENSG00000213619 | NDUFS3 | 372,098784 | 177,965739 | 155,921898 | 0,47827552 | 0,00440553 | 0,41903361 | 0,00901272 |
| ENSG00000139946 | PELI2 | 65,4338228 | 1,59173861 | 13,4467984 | 0,02432593 | 0,00453686 | 0,20550226 | 0,01939437 |
| ENSG00000184384 | MAML2 | 300,408584 | 85,2449007 | 114,091773 | 0,2837632 | 0,00458689 | 0,37978866 | 0,03440722 |
| ENSG00000134905 | CARS2 | 158,907733 | 10,8428122 | 49,8969489 | 0,06823338 | 0,00547621 | 0,3139995 | 0,02689644 |
| ENSG00000131269 | ABCB7 | 143,563571 | 19,2765199 | 50,6979546 | 0,13427167 | 0,00603154 | 0,35313941 | 0,03578281 |
| ENSG00000133106 | EPSTI1 | 1150,70886 | 552,333455 | 290,557797 | 0,47999409 | 0,00692409 | 0,25250331 | 0,00062848 |
| ENSG00000151136 | BTBD11 | 162,474411 | 94,9841988 | 51,2207355 | 0,58461021 | 0,00788463 | 0,31525417 | 0,02235092 |
| ENSG00000099899 | TRMT2A | 190,202131 | 27,7783043 | 12,7697276 | 0,14604623 | 0,00824233 | 0,06713767 | 0,00471173 |
| ENSG00000064490 | RFXANK | 275,05538 | 43,9146356 | 39,681674 | 0,15965743 | 0,00932798 | 0,14426794 | 0,00699375 |
| ENSG00000157916 | RER1 | 398,119848 | 192,47981 | 175,016106 | 0,48347203 | 0,01167829 | 0,43960658 | 0,0169765 |
| ENSG00000183751 | TBL3 | 90,4091695 | 17,9762693 | 34,1271911 | 0,19883237 | 0,01178078 | 0,37747489 | 0,04162642 |
| ENSG00000120875 | DUSP4 | 209,874289 | 24,6030937 | 9,32611699 | 0,11722776 | 0,01240733 | 0,04443668 | 0,00687208 |
| ENSG00000111481 | COPZ1 | 357,397052 | 140,835732 | 87,2291388 | 0,39405958 | 0,01344315 | 0,24406787 | 0,00656805 |
| ENSG00000198931 | APRT | 589,593449 | 342,471946 | 237,800295 | 0,58086118 | 0,01390169 | 0,40332927 | 0,02085269 |
| ENSG00000198646 | NCOA6 | 182,072571 | 54,5522654 | 57,1548136 | 0,29961825 | 0,01411414 | 0,31391227 | 0,00811549 |
| ENSG00000079616 | KIF22 | 206,377925 | 75,0898821 | 43,267647 | 0,36384648 | 0,01508284 | 0,20965249 | 0,01309665 |
| ENSG00000010626 | LRRC23 | 61,0594127 | 0 | 0 | 0 | 0,01575577 | 0 | 0,01575577 |
| ENSG00000138629 | UBL7 | 229,554369 | 72,0072778 | 46,9157671 | 0,31368289 | 0,01685894 | 0,20437758 | 0,0082534 |

| | | | | | | | | |
|-----------------|-----------|------------|------------|------------|------------|------------|------------|------------|
| ENSG00000122641 | INHBA | 556,254188 | 171,178228 | 222,580157 | 0,30773382 | 0,01758015 | 0,40014109 | 0,01859276 |
| ENSG00000139629 | GALNT6 | 189,622328 | 26,332544 | 43,5244582 | 0,13886837 | 0,01819785 | 0,22953235 | 0,02824244 |
| ENSG00000234663 | LINC01934 | 256,522135 | 61,4358085 | 74,1082588 | 0,23949516 | 0,01974883 | 0,28889616 | 0,00932596 |
| ENSG00000167550 | RHEBL1 | 51,7144787 | 7,96510415 | 0 | 0,15402078 | 0,0210976 | 0 | 0,0043738 |
| ENSG00000089327 | FXYD5 | 423,541897 | 185,702947 | 190,063978 | 0,43845236 | 0,02291935 | 0,44874894 | 0,03380467 |
| ENSG00000119777 | TMEM214 | 164,038013 | 61,9057325 | 10,2143186 | 0,3773865 | 0,02323601 | 0,062268 | 0,00080537 |
| ENSG00000136937 | NCBP1 | 157,764589 | 20,4632075 | 20,7662067 | 0,12970723 | 0,02354938 | 0,13162781 | 0,02413085 |
| ENSG00000105287 | PRKD2 | 389,14391 | 207,377701 | 149,528859 | 0,53290748 | 0,0237207 | 0,3842508 | 0,00353778 |
| ENSG00000106178 | CCL24 | 171,080368 | 2,31525616 | 0 | 0,01353315 | 0,02389884 | 0 | 0,02258917 |
| ENSG00000260032 | NORAD | 602,729154 | 233,284288 | 246,426497 | 0,38704663 | 0,02447802 | 0,40885113 | 0,01986862 |
| ENSG00000204899 | MZT1 | 86,1809023 | 24,9457777 | 15,0994275 | 0,2894583 | 0,02554405 | 0,17520619 | 0,015011 |
| ENSG00000257119 | EEF1B2P4 | 0,57218962 | 0 | 0 | 0 | 0,02557676 | 0 | 0,02557676 |
| ENSG00000276168 | RN7SL1 | 442,26816 | 89,5122576 | 122,540268 | 0,20239363 | 0,02629894 | 0,27707233 | 0,04125 |
| ENSG00000149923 | PPP4C | 264,870311 | 103,062383 | 103,342433 | 0,38910508 | 0,02729211 | 0,39016239 | 0,0417688 |
| ENSG00000119285 | HEATR1 | 242,322441 | 123,402423 | 81,5119043 | 0,50924884 | 0,02965932 | 0,33637786 | 0,03099973 |
| ENSG00000129484 | PARP2 | 63,4042115 | 0 | 0 | 0 | 0,02967919 | 0 | 0,02967919 |
| ENSG00000145996 | CDKAL1 | 265,897237 | 84,6000922 | 113,958126 | 0,31816838 | 0,03029757 | 0,42857958 | 0,04740999 |
| ENSG00000101246 | ARFRP1 | 88,6796355 | 120,242289 | 1,45478177 | 1,35591772 | 0,03054057 | 0,01640491 | 5,868E-05 |
| ENSG00000174780 | SRP72 | 637,077334 | 423,064158 | 306,412892 | 0,66407033 | 0,03214964 | 0,48096656 | 0,00083982 |
| ENSG00000197020 | ZNF100 | 23,3634661 | 0 | 0 | 0 | 0,03368603 | 0 | 0,03368603 |
| ENSG00000156050 | FAM161B | 38,4965394 | 0 | 0,58191271 | 0 | 0,03596311 | 0,01511597 | 0,0380802 |
| ENSG00000172183 | ISG20 | 1408,13542 | 942,360103 | 490,162798 | 0,66922548 | 0,03967294 | 0,34809351 | 0,00094244 |
| ENSG00000089639 | GMIP | 285,878343 | 117,529302 | 106,001341 | 0,41111649 | 0,04112767 | 0,37079179 | 0,0489591 |
| ENSG00000042286 | AIFM2 | 44,4655606 | 0 | 0 | 0 | 0,04227435 | 0 | 0,04227435 |
| ENSG00000159496 | RGL4 | 105,542189 | 23,19408 | 15,5398885 | 0,21976122 | 0,0459065 | 0,14723864 | 0,02363417 |
| ENSG00000090104 | RGS1 | 283,675981 | 79,3925329 | 37,0005518 | 0,27987048 | 0,04687639 | 0,13043244 | 0,02304922 |
| ENSG00000267508 | ZNF285 | 53,049637 | 0 | 0 | 0 | 0,04808685 | 0 | 0,04808685 |

Supplemental Table 8: Fold change of gene expression in parallelly regulated genes in naïve and total NaCl-stimulated CD8⁺ T cells

| | Present dataset | | Scirgolea et al., NI 2024 | Soll et al., NI 2024 |
|-------------------|-----------------|------------|---------------------------|----------------------|
| | + NaCl | + Urea | | |
| PRRG4 | 337,901087 | 287,577694 | 10,6642334 | 13,2645057 |
| DBNDD2 | 172,988444 | 0 | 2,41606905 | 2,48922358 |
| SLC39A8 | 94,1702244 | 77,5988557 | 1,91977885 | 2,08940479 |
| SFMBT2 | 60,2946743 | 3,87034139 | 1,91017168 | 2,15037951 |
| PRKAG2-AS1 | 55,6120133 | 14,1912518 | 5,01874405 | 6,20530867 |
| POLR3H | 11,6193702 | 4,12424589 | 2,08744982 | 1,76045016 |
| AKAP1 | 11,1750188 | 2,56137882 | 1,9213477 | 2,10592686 |
| ASRGL1 | 9,74620903 | 3,63372511 | | 2,52446258 |
| SLC5A3 | 7,50885861 | 0,80153325 | 3,80782553 | 4,17571224 |
| CDK2AP1 | 6,86711778 | 2,60353674 | 4,3340837 | 4,37069266 |
| PGP | 5,43868172 | 1,7791412 | 2,01430044 | 2,12717662 |
| ATP1B3 | 4,72296029 | 3,49559895 | 2,2349978 | 2,44412373 |
| CTPS1 | 4,48172469 | 1,89497012 | 2,33193403 | 2,50116254 |
| RBFA | 4,30715139 | 6,09829002 | 2,16365987 | 2,23666201 |
| MSMO1 | 3,52038934 | 1,73479132 | 2,10970773 | 2,3630765 |
| MRPS6 | 3,04327773 | 0,47642416 | 3,4101951 | 3,78668743 |
| PRMT1 | 2,88189047 | 0,24736862 | 1,96641651 | 2,12451048 |
| JAK3 | 0,48123036 | 0,69635457 | 0,38160523 | 0,43048401 |
| CD27 | 0,40616222 | 0,41957845 | 0,41077339 | 0,51733069 |
| NUAK2 | 0,38500391 | 1,46560237 | 0,15126972 | 0,17068591 |
| KDM7A | 0,32656271 | 1,00667795 | 0,39577776 | 0,41724795 |
| TTC39B | 0,3080859 | 0,59181478 | 0,48727932 | 0,50847458 |
| LMBR1L | 0,00947101 | 1,53056758 | 0,44258554 | 0,49070632 |
| MEGF6 | 0 | 0,81012845 | 0,15315614 | 0,1766427 |

Supplemental references:

1. Naesens M, et al. The Banff 2022 Kidney Meeting Report: Reappraisal of microvascular inflammation and the role of biopsy-based transcript diagnostics. *Am J Transplant.* 2024;24(3):338–349.
2. Bräsen JH, et al. Macrophage density in early surveillance biopsies predicts future renal transplant function. *Kidney Int.* 2017;92(2):479–489.
3. Apaolaza PS, Petropoulou P-I, Rodriguez-Calvo T. Whole-Slide Image Analysis of Human Pancreas Samples to Elucidate the Immunopathogenesis of Type 1 Diabetes Using the QuPath Software. *Front Mol Biosci.* 2021;8:689799.
4. Bankhead P, et al. QuPath: Open source software for digital pathology image analysis. *Sci Rep.* 2017;7(1):16878.
5. Goldspink A, et al. Kidney medullary sodium chloride concentrations induce neutrophil and monocyte extracellular DNA traps that defend against pyelonephritis in vivo. *Kidney International.* 2023;104(2):279–292.
6. Hüsing AM, et al. Myeloid CCR2 Promotes Atherosclerosis after AKI. *J Am Soc Nephrol.* 2022;ASN.2022010048.
7. Ewels PA, et al. The nf-core framework for community-curated bioinformatics pipelines. *Nat Biotechnol.* 2020;38(3):276–278.
8. The Bioconda Team, et al. Bioconda: sustainable and comprehensive software distribution for the life sciences. *Nat Methods.* 2018;15(7):475–476.
9. Da Veiga Leprevost F, et al. BioContainers: an open-source and community-driven framework for software standardization. *Bioinformatics.* 2017;33(16):2580–2582.
10. Di Tommaso P, et al. Nextflow enables reproducible computational workflows. *Nat Biotechnol.* 2017;35(4):316–319.
11. Xu K, et al. Unique Transcriptional Programs Identify Subtypes of AKI. *JASN.* 2017;28(6):1729–1740.
12. Scirgolea C, et al. NaCl enhances CD8⁺ T cell effector functions in cancer immunotherapy. *Nat Immunol.* 2024;25(10):1845–1857.
13. Soll D, et al. Sodium chloride in the tumor microenvironment enhances T cell metabolic fitness and cytotoxicity. *Nat Immunol.* 2024;25(10):1830–1844.
14. Yokose T, et al. Dysfunction of infiltrating cytotoxic CD8⁺ T cells within the graft promotes murine kidney allotransplant tolerance. *J Clin Invest.* 2024;134(16):e179709.